Arab American University

Faculty of Graduate Studies

Structural and functional compatibility of a novel mutation Asp413Asn and the Gly420Arg mutation in the factor X gene.

By

Osayd Samer Zohud

Supervisor

Prof. Hisham Darwish

This thesis was submitted in partial fulfillment of the requirements for the Master's degree in

Molecular Genetics and Genetic Toxicology

January/2020

Structural and functional compatibility of a novel mutation Asp413Asnand the Gly420Arg mutation in the factor X gene.

By

Osayd Samer Fathi Zohud

Thesis was submitted and defended successfully on……

Members of the Thesis Committee:

1. Prof. Hisham Darwish
2. Dr. Zaidoun Salah
3. Dr. Fawaz Awad

Declaration

Here I declare that my MSc thesis entitled "Structural and functional compatibility of a novel mutation Asp413Asnand the Gly420Arg mutation in the factor X gene" is the result of my own research and was written independently with no other sources than quoted.

Osayd Samer Zohud

Signature: Osayd Samer Zohud

Date: 19/8/2020

Dedication

This thesis is dedicated to my beloved father, mother, siblings and grandmothers.

It is dedicated to my deceased grandfather Fathi, who waited desirously to hold my degree.

It is also dedicated to my grandfather Rushdi hoping he will get well soon by the time of dissertation

Osayd Samer Fathi Zohud

Acknowledgments

I would like to express my deepest gratitude to my supervisor Professor Hisham Darwish for the unlimited encouragement and support during my project starting from proposal writing until my dissertation. Dr. Hisham was a great source of experiences and valuable knowledge, I acquired from him the ability to design, perform experiments, and how to evaluate and interpret results to link things together to come up with conclusions and new hypotheses. I also learned how to be a member of a team in a scientific project. In addition to non-science topics I have learned about away from the field. Hisham was not only a great supervisor but a wonderful and cheerful friend.

I would also like also to thank Dr. Zaidoun Salah for kindly following the progress of my project and providing me with valuable ideas and suggestions. I would like also to thank him and his team at Al-Quds University (Mahmoud, Ahmad, Abrar and Sondos) for their hospitality and providing me with some materials and technical experience I needed for my project.

Special thanks to Mr. Husam Sallam for his technical assistance and support. I would like also to thank my colleagues and friends especially Sondos, Niveen and Rosemary for the cheerful time and collaboration.

I also want to express my greatest thankfulness and appreciation for my beloved Mother Nasreen, Father Samer and siblings Sura, Sama and Ahmad for their support and encouragement during this challenging Journey.

Abstract

Factor X is a vitamin k dependent serine protease; produced in the Liver and has a pivotal role in the coagulation cascade. It is activated by either extrinsic or the intrinsic pathways. It constitutes a major component of the prothrombinase complex, which converts prothrombin into thrombin. Factor X is encoded by a gene on chromosome 13 consisting of 8 exons encoding a 488 amino acids protein. More than 130 mutations have been reported in *F10* gene, represented mostly by missense mutations. FX deficiency is classified as decrease in level and function (type1) or only dysfunction (type2) of the protein.

Recently, two novel mutations were identified in the FX gene in our group, one a substitution (c.1237 G>A) leading to missense p.Asp413Asn mutation. Another missense mutation (p.Gly420Arg) in the *F10* gene (c.1258 G>A) was reported in a previous study. Our study aimed to understand the functional and structural implications of both missense mutations on FX protein.

The full-length wild type *F10* cDNA was obtained commercially and used to generate both indicated missense mutations using site directed mutagenesis. The wild type and mutant constructs were transfected in HEK293t cells. Western blot analysis of the lysates from transfected cells showed no significant reduction in the FX protein level in both mutants compared to the wild type. FX activity (prothrombin time) was measured in the media of transfected cells and showed significant lower activity of both mutants compared to the wild type. Wild type and mutants F10 mRNA levels were measured in transfected cells and showed no significant difference. Bioinformatic analysis showed the both Asp413 and Gly420 are highly conserved in the catalytic domain of the protein among different species which indicates that

both amino acids are crucial for FX protein activity. Molecular modeling analysis showed noticeable structural change in the protein. This change was more apparent in the Gly420Arg mutant than Asp413Asn mutant, which is predicted from the nature of amino acid change; however, both mutants were predicted to be damaging in the protein structure. This is consistent with the FX protein and mRNA levels and loss of FX activity described above.

Table of contents

List of tables

List of figures

1. Introduction

Hemostasis is a physiological process that takes place in the human body to stop bleeding at specific sites of vessel injury by the formation of a blood clot. Normally endothelial tissue provides an anticoagulant surface that prevents blood clotting. When a blood vessel is damaged some components of the subendothelial tissue are exposed to blood. This leads to the initiation of the two main processes of hemostasis to form a blood clot. These include platelet aggregation (Primary hemostasis) and Secondary hemostasis, which is the formation of insoluble cross-linked fibrin by a cascade of serine proteases. Factor X (FX) is a central vitamin K dependent serine protease involved in coagulation process, it is released in circulation from liver as a proenzyme and later activated in plasma. Factor X or Stuart-Prower factor, plays a central role in blood coagulation (links the extrinsic and intrinsic pathways). (Hoffbrand & H. Moss, 2011) (Chafa, 2009)

Coagulation system is a complex biological amplification system with negative feedback loops to ensure limited and localized activation in changing fibrinogen into fibrin. Fibrin clot is essential to support platelet plug at the site of injury converting primary platelet plug to more firm definitive plugs. (Hoffbrand & H. Moss, 2011)

Coagulation factors are either enzymes or coenzymes except for fibrinogen. All the enzymes are serine proteases except for Factor XIII. Coagulation process is dependent on three enzyme complexes each involves an enzyme, coenzyme in addition to phospholipid (PL) and calcium (Ca^{++}), the coagulation process includes extrinsic tenase complex (FVIIa, tissue factor(TF), PL and Ca^{++}), intrinsic tenase complex (IXa, VIIIa, PL and Ca^{++}) both activating FX and prothrombinase complex (Xa, Va, PL and Ca^{++}), which converts prothrombin to thrombin.

Thrombin generation occurs in two waves. An initiation phase which occurs at the site of injury following the exposure of TF expressed on fibroblasts of the adventitia and interaction with FVII forming extrinsic tenase complex, which in turn activates and FX. The intrinsic pathway which includes several other factors leads to the activation of FX followed by a common pathway leading to the conversion of fibrinogen to fibrin. As shown in figure 1.1. (Hoffbrand & H. Moss, 2011)

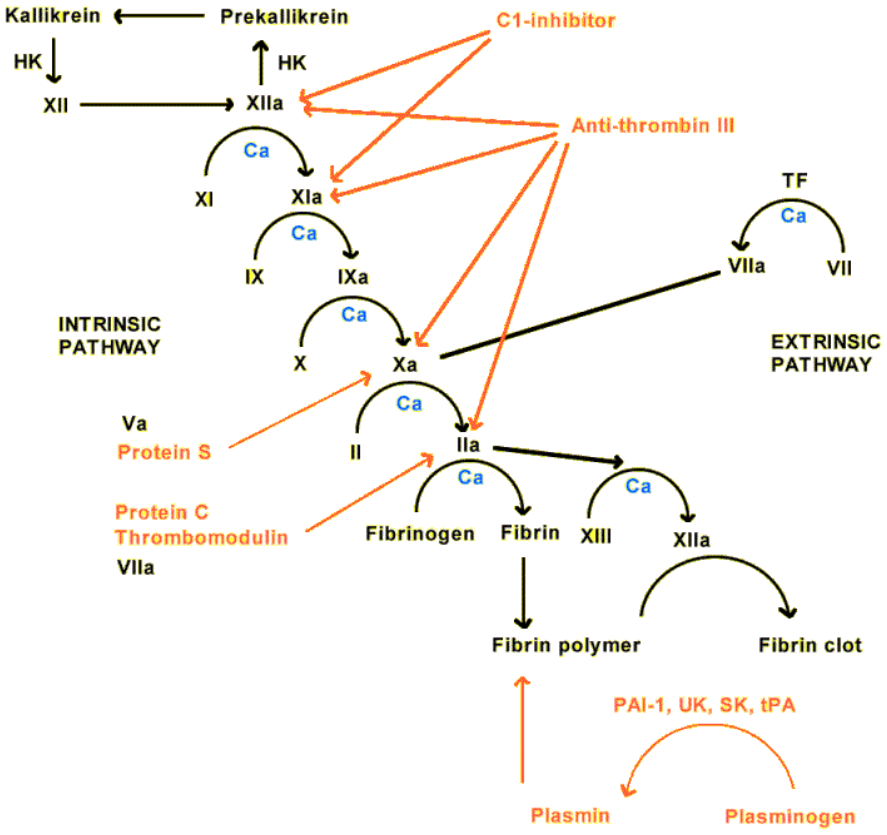

Figure 1.1: Coagulation cascade in vivo showing the extrinsic and intrinsic pathways and the central role of FX in this cascade.

(Perez-Pujol, 2012)

1.1. FX central role

Activated FX (FXa) is an essential component of the prothrombinase complex. Which also includes FVa, this complex is the only known physiological converter of prothrombin to thrombin, which in turn cleaves fibrinogen to form fibrin. FX could also be activated *in vitro* by a specific enzyme isolated from a snake venom (Russell's viper venom). (Shinohara, 2008) (Sun, 2016)

1.2. FX structure

The prepropeptide of FX is produced in hepatocytes as a single polypeptide chain; the first 40 amino acid residues, which contain the signal sequence (1-31) as shown in figure 1.3 to guide the secretion of the peptide, and the remaining segment (32-40) is cleaved by the proteolytic activity of Furin enzyme before secretion from liver into plasma. FX is found in blood consisting of two chains due to the endoproteolytic cleavage of Arg139 - Arg142, a heavy chain of about 45-kDa, and a light chain of 17-kDa are linked by a single disulfide bond, as shown in figure 1.2 (cys172-cys342). (Sun, 2016)

Other post-translational modifications include Gamma carboxylation of 11 glutamic acid residues in the N-terminus of the peptide also known as the ω-loop by a Liver microsomal vitamin K dependent carboxylase, Beta hydroxylation of aspartic acid 63 and N-glycosylation in two sites (Sun, 2016) (Padmanabhan, 1993).The light chain of FX contains two EGF like domains, that bind Calcium ions and Gamma carboxy glutamic acid (Gla) domain which binds Calcium with high affinity. A Ca^{++} dependent conformational change causes the exposure of hydrophobic Gla domain that will be inserted completely inside the PL and increases the catalytic activity of FX. It is conceived that the inner four Ca^{++} ions are essential for Gla optimal

folding for insertion inside the PL, while the outer Ca^{++} ions are needed to stabilize and anchor protein to PL by direct ionic interactions. Site directed mutagenesis studies suggests that Gla at positions 16,26 and 29 are the most essential for protein function. (Chafa, 2009) (Falls, 2001)

The heavy chain of FX consists of 52 amino acids activation peptide (183-234) (cleaved to activate FX by tenase complex), and the active peptidase domain (235-467) with active triad center composed of histidine 276, aspartic acid 322 and serine 419. These domains share high similar sequence identity with other vitamin k dependent clotting factors and serine proteases. (Nagaya, Congenital coagulation factor X deficiency: Genetic analysis of, 2018) (SUTTIE, 1993)

FX is activated by the cleavage of Arg234-Ile235 peptide bond, close to the amino terminus of the heavy chain under the proteolytic effect of either FVIIIa-FIXa complex (intrinsic pathway), or FVIIa-tissue factor complex (extrinsic pathway). The resulting free Isoleucine at the amino terminus of FX heavy chain folds inside the protease domain forming ionic interaction with aspartic acid close to serine 419. (Padmanabhan, 1993)

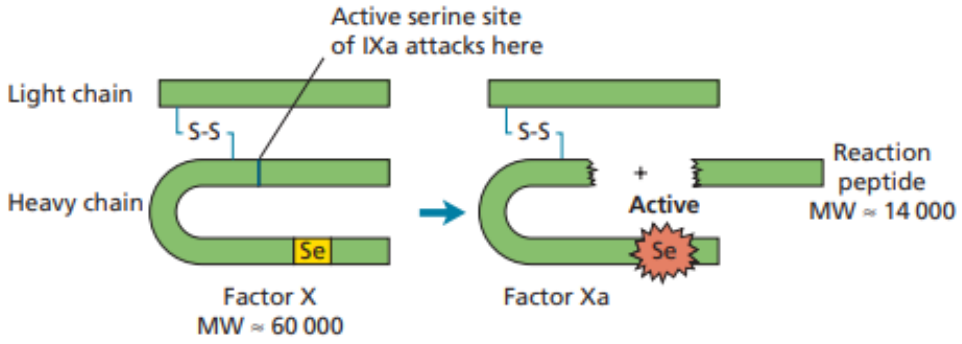

Figure 1.2: FX structure showing the heavy and the light chains linked by a disulfide bond and FX activation by FIX.

(Hoffbrand & H. Moss, 2011)

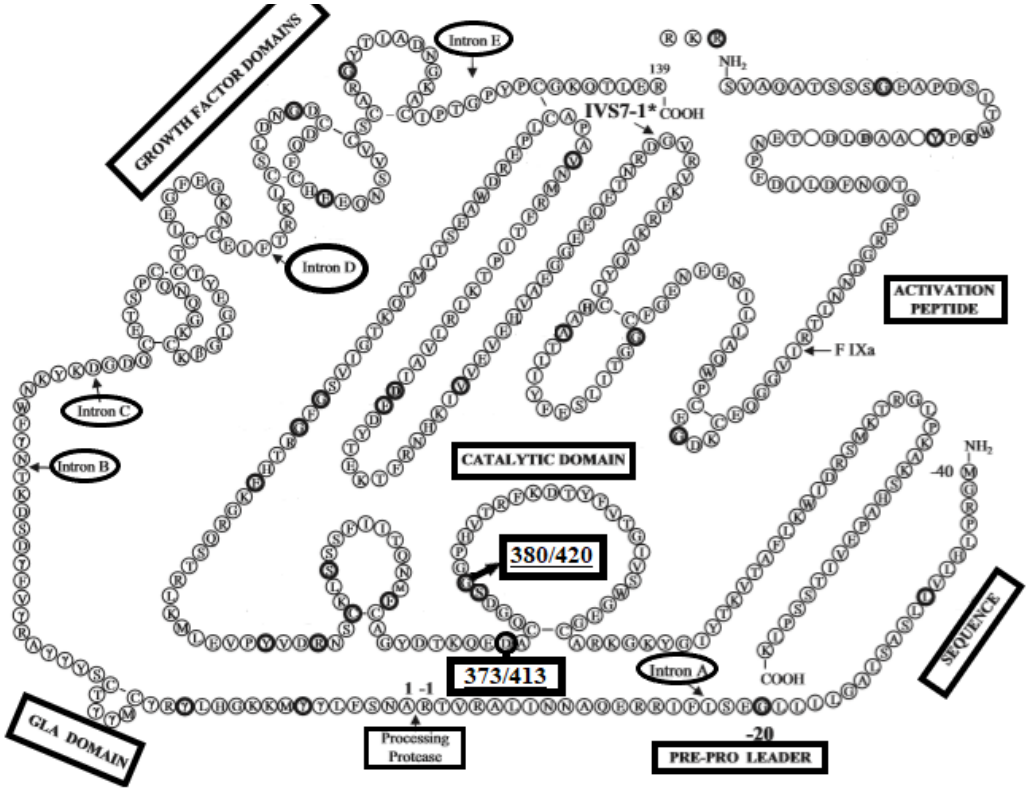

Figure 1.3: Detailed amino acids sequence of FX protein indicating all relevant functional domains.

(F. H. HERRMANN, 2008)

1.3. *F10* gene

FX is encoded by a gene located on the long arm of chromosome 13 (13q34), about 3kb downstream from the *F7* gene. The gene contains 8 exons and 7 introns spanning about 27kb as shown in figure 1.4. (Nagaya, et al., 2018). And the full length F10 cDNA was formerly isolated, cloned and characterized by P. LEYTUS et al. (Leytus, 1986) (Kaul, 1984)

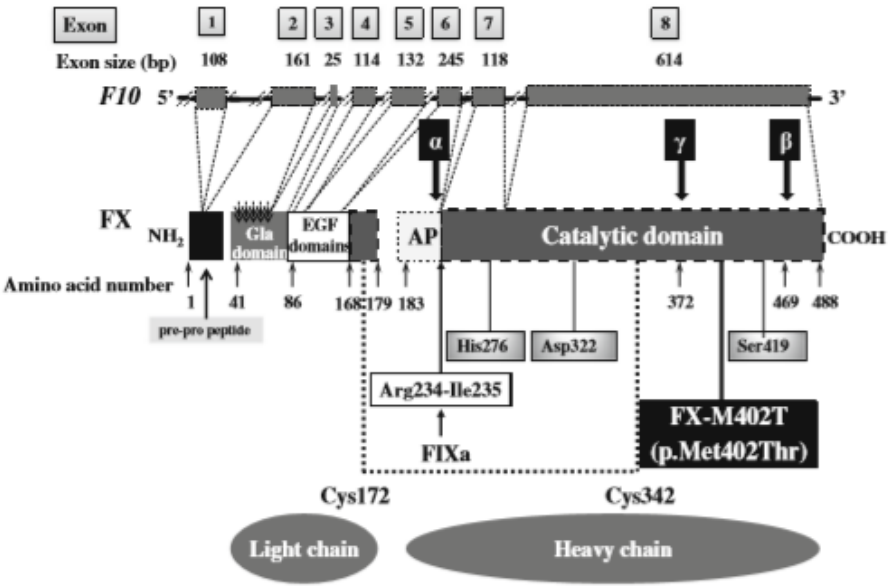

Figure 1.2: FX gene structure, showing the 8 exons, their sizes and the most important functional domains they code for.

(Chikasawa, et al., 2014)

1.4. FX deficiency

Inherited FX deficiency (FXD) is inherited as an autosomal recessive trait with general incidence of 1:1000000 and carrier frequency of 1:500. This incidence could be increased in populations with high consanguinity rates. (Sun, 2016). Mutations in the *F10* gene lead to congenital FX deficiency with approximately 135 reported mutations to date. Most of these mutations are missense mutations, others include insertion, deletion, frame shift and splice site mutations as described in table 1.1 according to the Human Gene Mutation Database.

Table 1.1: Mutations reported in *F10* gene

Mutation type	Number of mutations
Missense/nonsense	107
Small insertions	2
Small deletions	11
Small indels	1
splice site mutations	6
Gross deletions	8

(The Human Gene Mutation Database, 2019)

FX patients are diagnosed by prolonged prothrombin time (PT), a lab test that evaluates the extrinsic pathway, and prolonged activated partial thromboplastin time (aPTT) which tests the activity of the intrinsic pathway. (Karimi, 2008)

FX deficiency patients' clinical presentations represent the most severe type between other bleeding disorders, including hemarthrosis, epistaxis, easy bruising, excessive cord umbilical bleeding, gastrointestinal, pulmonary and central nervous system (CNS) bleeding. (Karimi, 2008)

The clinical phenotype and laboratory findings in FX deficiency are poorly corelated, therefore, these results only are not sufficient for the classification of clinical severity. The severity of FXD was only described as severe, moderate or asymptomatic phenotype. Multiple attempts were done to understand the variable bleeding tendencies based on the genotype, but this is not fully

understood due to limited available cases of FXD patients. (F. H. HERRMANN, 2008) (Karimi, 2008)

FXD is classified into two types based on plasma FX antigen level and enzymatic activity. Patients with decreased FX antigen and activity are stated as type I, while type II is characterized by deficient FX activity with normal or near normal FX level. (Sun, 2016)

In Palestine, due to high consanguinity rate we have congenital FXD rates of about 6:1000000 which is 6 times more than the international incidence rate. Recently, two novel mutations were identified in severe FXD patients, one a 5' Donor splice site mutation (IVS1+1G> T) and the second a missense mutation where Aspartic acid replaced with asparagine at position 413 (Asp413Asn). This shift from an acidic amino acid to a neutral polar amino acid is predicted to have a significant effect on the protein structure mainly the Na^+ binding loop (185-189). (Smoom, 2015)

Three recent studies investigated the molecular impact of other novel missense mutations identified using in vitro site directed mutagenesis technique. These include p.Ala275Val (Sun, 2016), Met402Thr (Chikasawa, et al., 2014) and p.Gly154Arg, p.Val236Met, p.Gly263Val, p.Arg387Cys, p.Gly406Ser and p.Val424Phe (Nagaya, 2018). Site directed mutagenesis technique was used also to study the structural and functional implications of other mutations and variants in other genes, for example the impact of p.Gly668Asp mutation in EPHA2 gene was reported previously, (Zhai, 2019). Similarly, the molecular impact of various mutations in the Interferon Beta gene were also studied using similar approach. (Norouzi , 2018)

1.5. Study aims and objectives

The structural and functional implications of the Asp413Asn and Gly420Arg in FX gene is not known. Studying molecular consequences of these mutations will provide valuable information that could direct novel therapeutic approach.

This study aims to understand the molecular impact of the Asp413Asn (c.1237 G>A) mutation on the transcription of the gene and the function of FX. And to assess the capacity of synthesis and secretion in the WT and Asp413Asn mutant proteins by western blotting.

2. Materials and Methods

2.1. Materials

Table 2.1 Chemicals and Reagents

Chemicals and reagents	Source
Agar	Peqlab
Agarose	hylabs
Ammonium persulfate (APS)	Sigma-Aldrich
Cycloheximide	Sigma-Aldrich
Dimethyl sulfoxide (DMSO)	Sigma-Aldrich
Ethanol, absolute	Bio Lab
Ethidium bromide	hylabs
Glycine	Sigma-Aldrich
HCl	Sigma-Aldrich
Isopropanol	Bio Lab
Kanamycin	Sigma-Aldrich
Methanol	Sigma-Aldrich
Penicillin/streptomycin (P/S)	Life Technologies
Phosphate-buffered saline (PBS)	Life Technologies
RPMI cell culture media	Life Technologies
Sodium dodecyl sulfate (SDS)	Life Technologies
Sodium hydroxide (NaOH)	Bio Lab
Tris ultrapure	Promega
TRI reagent	Sigma-Aldrich

Triton X-100	Sigma-Aldrich
TEMED	Sigma-Aldrich
Trypsin-EDTA 0.05%	Life Technologies
Tween 20	Sigma-Aldrich
Yeast extract	hylabs

Table 2.2: Consumables

Article	Specifications	Source
Eppendorf tubes	1.5 ml	Axygen
Cell culture dishes	10 cm	Greiner
Cell scrapers	1.7 cm blade	Biologix
Centrifuge tubes	15, 50 ml	Falcon
PCR reaction tubes	0.2 ml	Axygen
Pipette tips	10, 100, 200 1000 µl	Life gene
Pipette tips with filters	10, 100, 200 1000 µl	Life gene
Serological pipettes	5, 10, 25 ml	labForce

Table 2.3: kits

Kit	Application	Company
F10 cDNA expression vector	Transfection	Origene
QuikChange Lightning Site-Directed Mutagenesis Kit	Site-Directed Mutagenesis Kit	Agilent
NucleoSpin® Plasmid	Plasmid DNA	Macherey-Nagel

	purification	
PureLink™	Maxiprep plasmid purification from bacteria	Invitrogen
ViaFect	Transfection Reagent	Promega
Maxima First Strand cDNA Synthesis	cDNA synthesis	Thermo Scientific
SYBR™ Green PCR Master Mix	Real Time PCR	Thermo Scientific
Hemostat Thromboplastin-SI	PT	Human Diagnostics
Trans-Blot® Turbo™ Midi PVDF Transfer Packs	Western blotting	Bio-Rad
Human Factor X ELISA Kit	ELISA	Abcam

Table 2.4: Table of Cells used

Cells	**Description**
XL10-Gold	Ultracompetent Cells provided by site directed mutagenesis kit
DH5α	High-efficiency chemically competent cells for transformation
HEK293T	Immortalized human embryonic kidney cell line

Table 2.5: Primary antibodies

antibody against	Dilution in WB	Source	Cat. N.	Company
FX	1:5000	Mouse/Monoclonal	66753-1-Ig	Proteintech
GAPDH	1:10000	Rabbit/Polyclonal	ab8227	Sigma

Table 2.6: Horseradish peroxidase (HRP)-conjugated secondary antibodies for western blotting

Secondary antibodies against	Dilution	Source	Cat. N.	Company
Mouse	1:20000	Goat	A90-144P	BETHYL
Rabbit	1:20000	Goat	A120-101P	BETHYL

Table 2.7: Mutagenesis Primers

Oligonucleotide	Strand	Sequence (5'–3')
Asp413Asn	Forward	CCCTGGCAGGCATTCTCCTGCTTGGTG
	Reverse	CACCAAGCAGGAGAATGCCTGCCAGGG
Gly420Arg	Forward	AGGGGGACAGCAGGGGCCCGCAC
	Reverse	GTGCGGGCCCCTGCTGCTGTCCCCCT

Table 2.8: Real Time PCR Primers

Oligonucleotide	Strand	Sequence (5'–3')
F10 (for real time PCR and sequencing)	Forward	TGTCCAGCAGCTTCATCATC
	Reverse	GCGGTGACCTTGGTGTAGAT
β-actin (housekeeping gene)	Forward	TTCCAGCCTTCCTTCCTGGG
	Reverse	TTGCGCTCAGGAGGAGCAAT

2.2 Expression vector and mutagenesis.

2.2.1 Expression vector

A 6.3 kb plasmid containing *F10* cDNA was commercially provided from Origene (CAT#: RC208506) as shown in figure 2.1. The 1.5 kb *F10* gene cDNA was cloned downstream of a T7 promoter in the plasmid that also contained kanamycin resistance gene. Selection of bacterial cells which were transformed with the plasmid was done using Kanamycin containing media plates. The detailed sequence of *F10* cDNA was cloned in the plasmid vector as shown in figure 2.2.

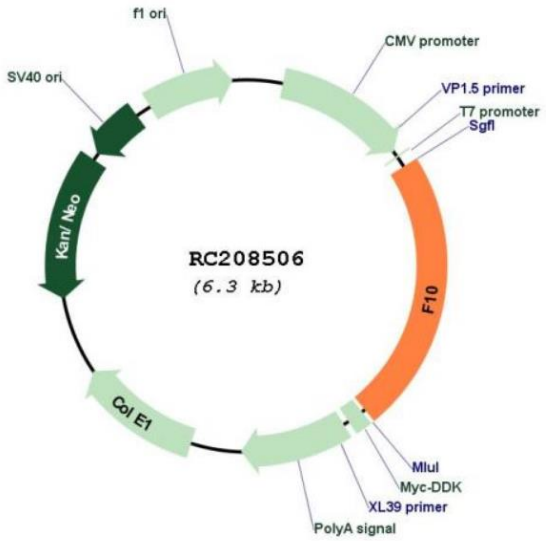

Figure 2.3: Circular map for RC208506 Plasmid housing the full *F10* length cDNA.

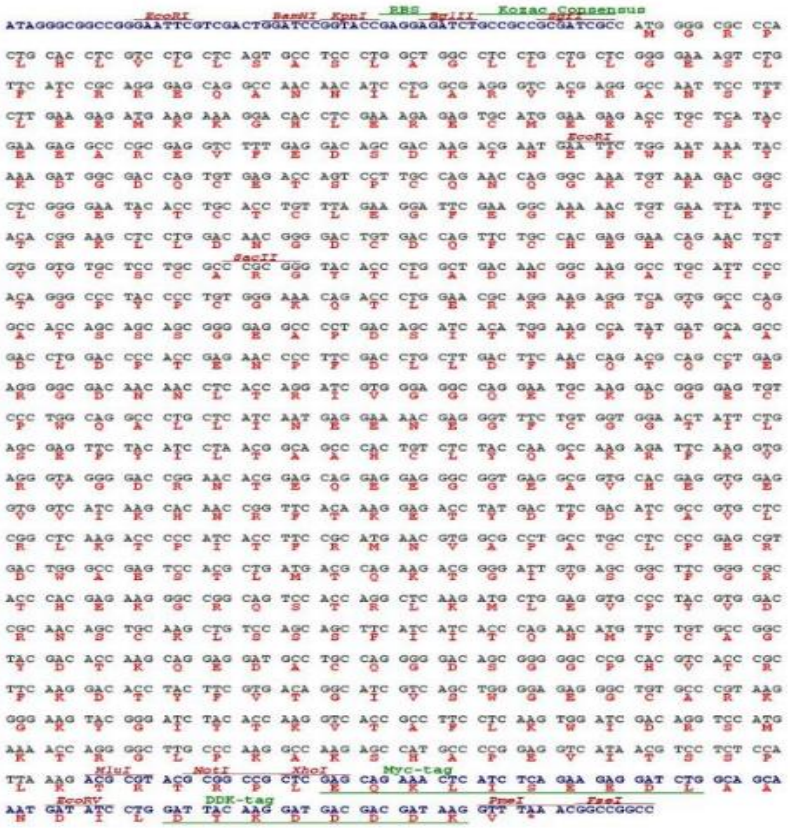

Figure 4.2: *F10* cDNA cloned in the vector

2.2.2 Site directed mutagenesis

Quick change lightning site directed mutagenesis was used to independently introduce two mutations in the FX cDNA sequence. The first (**Asp413Asn**), which was identified in a Palestinian severe FX deficiency patient resulting in an amino acid change from the negatively charged **Aspartic acid** to the neutral amino acid **Asparagine**, and the second mutant, (**Gly420Arg**), which was previously reported that causes a shift from the neutral amino acid **Glycine** to the positively charged **Arginine**. The Mutagenic primers were designed having the desired mutation in the middle of the primer flanked by complementary sequences. The web-based Quick-change Primer Design Program available on line was used for the indicated primers design as described in table 2.9.

https://www.chem.agilent.com/store/primerDesignProgram.jsp

Table 2.9: Mutagenic primers indicating the changed base

Mutation	Sequence (5'–3')
Asp413Asn	CCCTGGCAGGCAT**T**CTCCTGCTTGGTG
	CACCAAGCAGGAG**A**ATGCCTGCCAGGG
Gly420Arg	AGGGGGACAGC**A**GGGGCCCGCAC
	GTGCGGGCCCC**T**GCTGCTGTCCCCCT

The mutagenesis protocol.

- Primers were diluted to 125 ng/µl.
- The mutagenesis PCR reaction mixture was prepared as follows:

- 5 µl of 10× reaction buffer.
- 1 µl (10–100 ng) FX cDNA.
- 1 µl (125 ng) forward primer.
- 1 µl (125 ng) reverse primer.
- 1 µl dNTP mix.
- 1.5 µl Quick Solution reagent.
- 39.5 µl ddH_2O.
- Finally, 1 µl of Quick-Change Lightning Enzyme was added.

Table 2.10: The mutagenesis PCR protocol

Cycles	Temperature	Time
1	95	2 m
18	95	20 sec.
	60	10 sec.
	68	30sec./kb of plasmid (3:15)
1	68	5 m

Dpn I digestion.

The PCR reaction was centrifuged and preheated to 37C before the addition of 2 µl of Dpn I enzyme and incubated for five minutes at 37C to digest the paternal plasmid copies. DNA sequencing of the generated plasmids were done to confirm the intended nucleotide change.

Table 2.11: mutations confirmed by sequencing

Mutation	Asp413Asn	Gly420Arg
Wild type	CAGGAGGATGCCTGC	GACAGCGGGGGCCCG
Mutation seguence	CAGGAGAATGCCTGC	GACAGCAGGGGCCCG

2.3. Preparation of transfection grade plasmids.

2.3.1. Transformation of XL10-Gold ultracompetent cells.

- **Lysogeny broth (LB) was prepared as follows.**

  - 10g tryptone.
  - 5 g yeast extract.
  - 7.5g NaCl.
  - 1000 ml of ddH2O.

The media was autoclaved at 121C for 20 minutes followed by proper mixing.

- **Preparation of LB agar plates.**

  The following components were mixed as follows.

  - 10g tryptone.
  - 5 g yeast extract.
  - 7.5g NaCl.
  - 22g agarose.
  - 1000 ml of ddH_2O.

The media was autoclaved at 121C for 20 minutes.The mixture was left to cool to about 50C and 0.5 ml of 50 mg/ml Kanamycin stock solution was added to obtain final concentration of 25 ug/ml before pouring into petri dishes.

- **Bacterial transformation.**

The XL 10-Gold ultracompetent cells provided by the site directed mutagenesis kit were transformed with the plasmids containing the two generated mutant cDNA sequences Asp413Asn (G>A) and Gly420Arg (G>A) according to the following protocol:

- XL 10-Gold ultracompetent cells were thawed on ice.
- Aliquots of 45 µl of XL 10-Gold ultracompetent cells were added for each reaction.
- 2 µl of β- mercaptoethanol (provided by the kit) was added and incubated on ice for 2 minutes.
- 2 µl of Dpn I treated plasmids were added to the transformation reaction.
- The transformation reactions were mixed gently and incubated on ice for 30 minutes.
- Heat shock for 30 seconds at 42C in water path.
- Immediately incubate on ice for 2 minutes.
- Preheated LB (0.5 ml) was added and incubated with shacking for 1 hour.
- 250 µl of each transformation reactions were plated in a prelabeled LB agar plates containing 25 ug/ml kanamycin, and incubated overnight at 37C.

2.3.2 Plasmid purification by mini prep.

Four colonies were selected from each plate of the transformed bacteria for plasmids purification using MN NucleoSpin® Plasmid Easy Pure protocol as follows.

- The selected colonies were eluted by150 µL of buffer A1.

- Plasmid DNA was liberated from bacterial cells using 250 µL of buffer A2, the mixture was mixed gently to avoid contamination with genomic DNA.
- Buffer A3 was added (350 µL) to enhance plasmid DNA silica gel binding.
- Eppendorf tubes were centrifuged for 3 minutes at full speed to pellet proteins, genomic DNA, and cell debris.
- Supernatant was loaded in NucleoSpin® Plasmid Easy Pure Column and assembled with the collection tube.
- The tubes were centrifuged for 30s at 1000 x g, the flow-through was discarded
- The column was washed with AQ buffer supplemented with ethanol.
- Centrifugation for 1 minute at 12,000 x g
- The NucleoSpin® Plasmid Easy Pure Column was placed in a 1.5 ml collection Eppendorf tube. 50 ul of elution buffer was gently added and incubated for 1 minute at room temperature, then centrifuged for 1 minute at 12,000 x g.
- The amount and purity of collected plasmid DNA in collection tubes were evaluated using nanodrop, presented in table 2.13.

Table 2.12: NucleoSpin Plasmid EasyPure protocol

	NucleoSpin® Plasmid EasyPure	
1 Cultivate and harvest bacterial cells		12,000 x *g*, 30 s
2 Cell lysis		150 µL Buffer A1 250 µL Buffer A2 RT, up to 2 min 350 µL Buffer A3
3 Clarification of the lysate		>12,000 x *g*, 3 min
4 Bind DNA		Load supernatant 1,000–2,000 x *g*, 30 s
5 Wash and dry silica membrane		450 µL Buffer AQ >12,000 x *g*, 1 min
6 Elute DNA		50 µL Buffer AE RT, 1 min >12,000 x *g*, 1 min

Table 2.13: purified plasmids concentrations

Colony No.	Asp413Asn	Gly420Arg
1	42 ug/ml	67 ug/ml
2	54 ug/ml	66 ug/ml
3	53 ug/ml	52 ug/ml
4	54 ug/ml	35 ug/ml

In order to provide transfection grade plasmid concentration (sufficient amount), the provided WT plasmid in addition to Mutant 1 (Asp413ASN) and mutant 2 (Gly420Arg) plasmid constructs were transformed in DH5α according to the following protocol:

- Chemically produced DH5α was thawed on ice for 10-15 minutes.

- 20 ng of plasmid were added to 50 ul of bacterial suspension incubated on ice for 30 minutes.
- The cells were heat shocked for 1 minute at 42C and returned to ice for 5 minutes.
- The bacterial cells were incubated for 5 minutes at room temperature followed by addition of 1 ml of LB broth and then incubated for 1 hour at 37C with shaking.
- The cells were centrifuged for 1 minute at 10,000 rpm.
- The supernatant was discarded and the pellet was resuspended with 0.1 ml LB
- The pellet was streaked on LB agar plates containing 25 ug/mL Kanamycin and incubated overnight.
- colony from each transfection experiment was transferred to a 250ml bottle of LB broth with 25 ug/mL Kanamycin, and incubate at 37C with shacking overnight.

2.3.3 Maxi prep

The next day, Pure Link HiPure Plasmid Filter DNA Purification Kit was used to purify plasmids from transformed bacteria.

- 30 ml of equilibration buffer 1 (EB1) was added to HiPure Filter Maxi Column and allowed to drain by gravity.
- Bacterial cells grown in 250 ml LB broth with Kanamycin were centrifuged at 4000 x g for 10 minutes.
- The pellet was resuspended in resuspension buffer 3 (R3) with RNase.
- The cells were lysed with 10 ml lysis buffer 7 (L7) and mixed gently by inverting until a homogenous solution formed.

- After 5 minutes, 10 ml of precipitation buffer N3 was added, and mixed gently until the solution becomes homogenous.
- The precipitated cell lysate was transferred to the equilibrated filter and let run by gravity flow and the flow through was discarded.
- The maxi column was washed with 50 ml of washing buffer and the flow through was discarded.
- 15 ml of elution buffer were added to the maxi column the flow through was collected in sterile 50 ml tube.
- 10.5 ml of isopropanol was added to elution tube and the tube was centrifuged at 15,000 x g for 30 minutes at 4C.
- The supernatant was discarded and 5 ml of 70% ethanol was added.
- The tube was centrifuged at 15,000 x g for 5 minutes at 4C.
- The supernatant was removed and the pellet was left to air dry for 10 minutes.
- The pellet was resuspended with 200ul-500ul based on the pellet size.
- The amount of plasmid purified was measured using nanodrop. presented in Table 2.14.

Table 2.14: maxi prep plasmids concentrations

Name	Concentration
Wild Type	934.2 ng/ul
Mutant 1	839 ng/ul
Mutant 2	332.7 ng/ul

- DNA Sequencing was done for the maxiprep plasmids to confirm the indicated nucleotide sequence change.

2.4. Culturing, passaging and maintenance of HEK293T cells.

The cryovials of HEK293T cells were thawed quickly to 37C in a water bath, and sufficient amount of RPMI media supplemented with 10% FBS was added. The cells were seeded in 10 cm Petri dishes and incubated at 37C and 5% CO_2. The media was exchanged every 48 hours.

HEK293T cells were passaged after reaching 80% confluency. This was done by removing old culture media, washing cells with PBS and 1 ml of 0.05% EDTA-Trypsin was added for about 5 minutes until the cells detach and round up. Then appropriate amount of media was added (about 7.5 ml) and the cells were split into 2 plates.

In case of splitting before transfection, cells were diluted (1:10 were chosen) and transfection was done when they reached acceptable confluency (50-60%).

2.5. Transfection of HEK293T cells

Viafect transfection regent was stored at 4^{o} C and used for the transfection step.

- Viafect transfection regent was allowed to equilibrate at room temperature and then mixed properly.
- The culture media was exchanged 2 hrs before transfection where 90% of the media volume was added to the cells.
- 10 ug of plasmid DNA from each of the three purified plasmids by maxi prep was mixed with 20 ul of viafect transfection reagent in Eppendorf tubes.

- Serum free media was added to a final volume of 1 ml, the mixture was allowed to set for 10 minutes (not to exceed 20 minutes) and then distributed evenly over the plate with swirling to ensure proper mixing.
- The transfection process was done in duplicates for each plasmid. (one plate for RNA extraction and the other for cell lysate preparation).
- After 48 hours, the supernatant media was collected in prechilled labeled tubes, centrifuged to get rid of cell depress, and stored at -80C until used, cells were lysed or treated with the protein synthesis inhibitor cycloheximide (100 μg/mL) for 3 hrs. Cell lysates were subjected to immunoblotting..

2.6. Protein biochemical analysis

2.6.1. Lysing with RIPA Lysis buffer

Radioimmunoprecipitation assay lysis buffer was usually used in immunoprecipitation assays and chromatin immunoprecipitation due to its extreme denaturing activity (LC, 2008). It is preferred to use fresh prepared RIPA buffer, therefore the buffer was prepared the day before lysing procedure based on the following recipe and stored at 4C.

Table 2.15: RIPA lysis buffer recipe

Stock	Volume	[Final]
5 M NaCl	3 mL	150 mM
0.5 M EDTA, pH 8.0	1 mL	5 mM
1 M Tris, pH 8.0	5 mL	50 mM
NP-40 (IGEPAL CA-630)	1 mL	1.0%
10% sodium deoxycholate	5 mL	0.5%
10% SDS	1 mL	0.1%
dH2O	84 mL	

Just before lysis of the transfected cells, ice cold RIPA lysis buffer was mixed with protease inhibitor cocktail to prevent protein degradation.

Table 2.16: protease inhibitor added to RIPA lysis buffer

Stock	Volume	[Final]
Ice cold RIPA Lysis Buffer	10 mL	
100X Halt Protease Phosphatase Inhibitor CockTail	0.1 mL	1X

Cell lysing was done on ice. To achieve this, 0.5 ml of ice cold RIPA lysis buffer was used to lyse adherent cells with about 80% confluency on petri dishes with the aid of cell scrapers, the cells were scraped and collected in Eppendorf tubes and centrifuged at 13,000 x g for 5 minutes to get rid of cell depress. Cell lysates were kept at -80C for later use.

2.6.2 Protein separation and immunoblotting by western blot analysis:

Sodium dodecyl sulfate (SDS) polyacrylamide gel electrophoresis (SDS-PAGE) was done to separate proteins in cell lysate samples. Protein levels per cell lysate was measured by Bradford assay and equal quantities of protein were mixed with 4X sample buffer and incubated at 95C for 10 minutes.

4X sample buffer was prepared by mixing the following components:

- 1.26 ml of 1 M Tris/HCl (pH 6.8).
- 5.4 ml of 75% Glycerol.
- 460 mg SDS.
- 100 µL Bromophenol Blue.
- 2.8 mL H_2O.
- 20 µL DTT.
- 50 µL β-mercaptoethanol.

15% SDS-polyacrylamide gel preparation.

The following components were mixed in a 50 mL falcon tube to prepare the separation gel after the gel casting apparatus was assembled:

- 3.2 mL of 40% Bis-acrylamide.
- 1.1 mL of 3M Tris/HCl (pH 8.8).
- 4.1 mL ddH_2O.
- 85 µL of 10% SDS.
- 60 µL of 10 APS.
- 7.5 µL TEMED.

Pour the mixture in the casting apparatus leaving enough space for the stacking gel and the comb, add a layer of isopropanol on top of the separation gel to remove air bubbles and keep the gel from drying out and leave for 30 minutes for the gel to completely polymerize.

Remove isopropanol and wash the remaining with distilled water.

The stacking gel was prepared by mixing the following components:

- 0.28 mL of 40% Bis-acrylamide.
- 0.38 mL of 3M Tris/HCl (pH 8.8).
- 1.93 mL ddH_2O.
- 25 µL of 10% SDS.
- 12.5 µL of 10 APS.
- 6.25 µL TEMED.

Pour the staking gel on top of the separation gel, add coombs and leave for 30 minutes for the gel to completely polymerize. Mount the gel in the electrophoresis apparatus and fill the chamber with running buffer.

10X running buffer was prepared previously as follows:

- 30 g Tris Base.
- 144 g Glycine.
- 10 g SDS.
- Add ddH_2O to a final volume of 1 L.

Boiled samples (20 µL) and the molecular weight markers were loaded in the wells of SDS-polyacrylamide gel. The samples were electrophoresed at 80 volts for 30 minutes then on 120 volts for 1.5-2 hrs.

Proteins were blotted to a nitrocellulose membrane for 7 minutes using transblot turbo. The membrane was blocked by incubation with 5% skim milk on a rocking platform for 30 minutes. After blocking, membranes were incubated with primary antibodies overnight at 4C on a rocking platform.

The next day the membrane was washed with 10 mL TTBS (Tween-Tris Buffered Saline) three times (10 minutes each) before membrane incubation with anti-mouse

secondary antibodies with Horseradish Peroxidase for 2 hrs. Signal development was obtained after incubation in Clarity Western ECL(enhanced luminol-based chemiluminescent) Substrate (Bio-Rad) and signal development was obtained by gel documentation system.

2.7. Protein activity

Recombinant FX activity was tested by one stage prothrombin time. Media collected over the cells was concentrated 10-fold by speed-vac system and FX deficient plasma was used to provide the indicated FX factors for the clotting reaction. The plasma was mixed with concentrated conditioning media in 1:1 and was tested as normal human plasma using HumaClot junior blood coagulation machine.

2.8. Protein level

Recombinant FX level was tested by ELISA using Human Factor X ELISA Kit (Abcam). Fifty (50)ul of each standards and samples were added to pre-coated wells with human FX antibodies for 2 hrs. The wells were by washed using the washing buffer provided by the kit, 50 ul FX biotinylated antibodies were added per well, incubated for 1 hr. and washed again. Next, 50 ul 1X SP conjugate Ab was added to each well for 30 minutes followed by a washing step and 50 ul of chromogen substrate was added to each well. After the addition of 50 ul of stop solution, the plate was read by micro-plate reader where the color formed in each well is directly proportional with FX level in the sample.

2.9. RNA and *F10* expression level

2.9.1 RNA extraction.

RNA was extracted from monolayer adherent cells. After the media was removed, cells were lysed using 1ml TRI reagent per 10 cm^2 plate, collected in pre labeled Eppendorf tubes, and allowed to stand for 5 minutes at room temperature.

For each tube, 0.2 ml chloroform was added, vortexed for 15 seconds and left to stand for 5–15 minutes at room temperature. The mixture was centrifuged at 12,000 x g for 15 minutes at 4^o C. The mixture was separated into 3 layers, and the aqueous supernatant colorless layer containing RNA was transferred to a new prelabeled Eppendorf tube. For each tube, 0.5 ml ice cold 2-propanol was added, allowed to stand for 5-10 minutes at room temperature before centrifugation at 12,000 x g at 4^o C. The RNA was detected as a white precipitate in the bottom of the tube.

The supernatant was discarded and the RNA pellet was washed with 1 ml 70% ethanol and centrifuged at 7,500 x g for 5 minutes at 4^o C. The supernatant was removed and the RNA pellet was allowed to air dry for 5 minutes.

2.9.1. cDNA synthesis.

cDNA was synthesized using maxima cDNA synthesis kit as follows.

Table 2.17: cDNA reaction mix

5X Reaction Mix	4 ul
Maxima Enzyme Mix	2 ul
Template RNA	1 ug
Nuclease free water	Complete to 20 ul

The reaction was done in a PCR machine and the mixtures were incubated at 25^{o} C for 10 minutes followed by 50^{o} C for 15 minutes. The reaction was terminated at 85^{o} C for 5 minutes.

2.9.2. Real time PCR

The real time PCR was performed using 2X SYBR™ Green PCR Master Mix. The cDNA previously synthesized was diluted 1:1, the primers were diluted to 10 µM and two master mixes were done for both the FX gene and a house keeping gene as follows:

Table 2.18: RT PCR mix scheme

Component	Volume for 20 µl reaction
2X SYBR Green PCR master mix	10 µl
Forward Primer	0.5 µl
Reverse Primer	0.5 µl
cDNA (1:10 diluted)	3 µl
Nuclease free water	6 µl

The samples were arranged in a 96 well real time PCR plate, sealed, and centrifuged. The reaction was performed using APPLIED BIOSYSTEMS 7500 RT PCR machine as follows:

Table 2.19: RT PCR program

Step	Temperature (C)	Time	Cycles
Initial denaturation	95	15	1
Denaturation	95	15	40
Annealing	60	60	
Elongation	60		
Dissociation curve	95	15	1

2.10. In silico analysis of amino acid change

The impact of the two mutations of interest on the FX protein (uniport code P00742) was studied using three bioinformatic tools PolyPhen-2. (http://genetics.bwh.harvard.edu/pph2/) (Adzhubei IA, 2010), SIFT (http://provean.jcvi.org/index.php) (Yongwook Choi, 2012) and HOPE (https://www3.cmbi.umcn.nl/hope/) (Hanka Venselaar, 2010).

The conservation of the studied mutations was investigated by multiple sequence alignment tool from NCBI, COBALT (https://www.ncbi.nlm.nih.gov/tools/cobalt/re_cobalt.cgi) (NCBI, 2019).

3. Results

3.1. Mutagenesis results.

The generated $FX^{Asp413Asp}$ and $FX^{Gly420Arg}$ mutants were confirmed by sequencing of the 200 bp segment containing both of the indicated mutations after PCR amplification using primers described in table 2.8.(the PCR amplification products are shown in figure3.1) The sequences for each mutation compared to the wild type sequence are presented in Figure 3.3.A and 3.3.B for $FX^{Asp413Asp}$ and $FX^{Gly420Arg}$ respectively.

The full-length sequence of *F10* cDNA was also confirmed using sequencing primers provided with the vector by origene as shown in figure 3.2.

Figure 3.5: The 200bp amplified DNA fragment used to confirm mutation sequence.

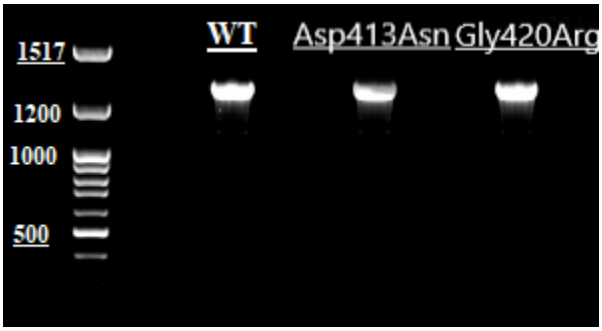

Figure 3.2: *F10* cDNA full-length sequence was confirmed and sequenced to confirm nucleotide change.

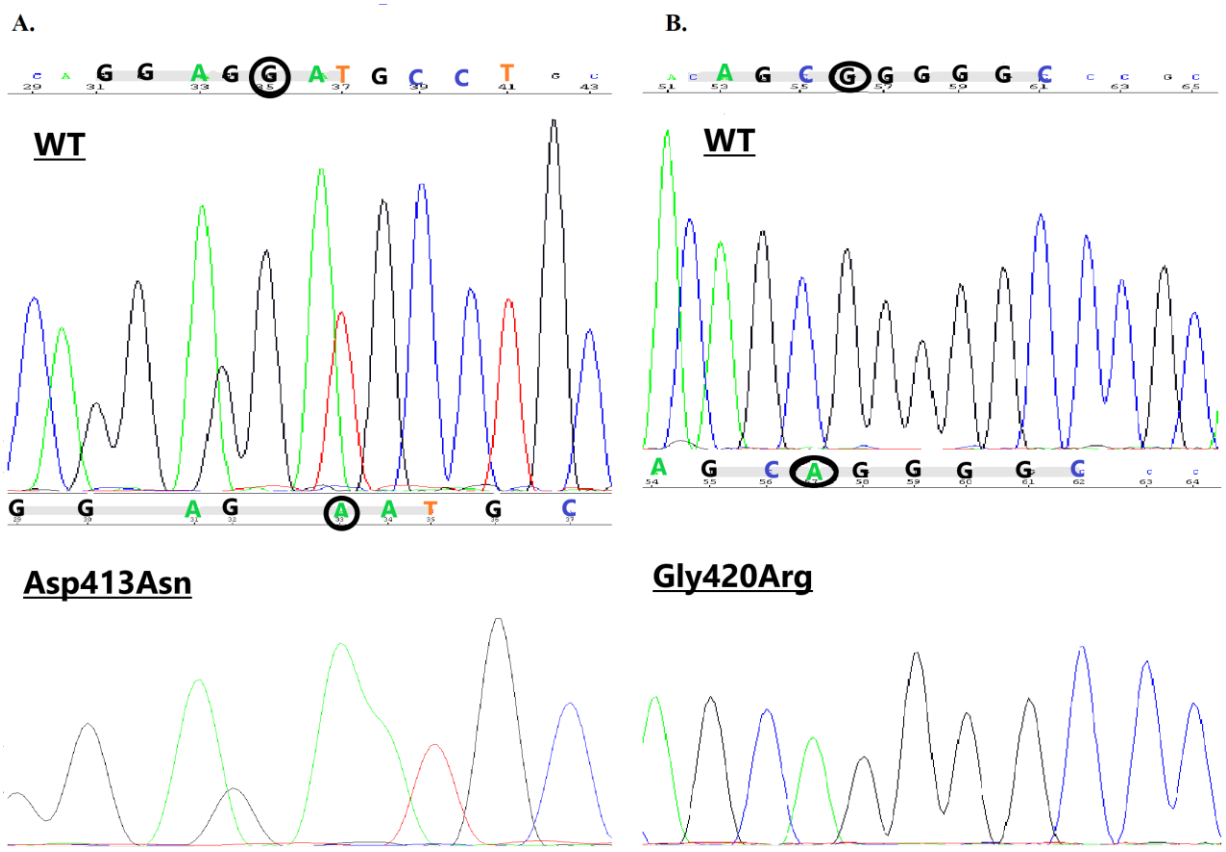

Figure 3.3: sequence confirmation for both mutants (A) shows the nucleotide change G>A In the Asp413Asn mutant compared to the wild type sequence (B) shows the G>A nucleotide change in the Gly420Arg compared to the wild type sequence

3.2. Recombinant FX level in cell lysates of transient transfected cells.

The level of FX protein was evaluated in cell lysates by both SDS-PAGE and ELISA to assess the capacity of synthesis and secretion of the both mutants, and WT FX recombinant proteins.

3.2.1. SDS-PAGE:

In order to investigate the expression of the indicated mutants and the expected protein size, equal amounts of protein from cell lysate were loaded on an SDS-PAGE and processed with western blotting analysis, The FX protein bands were detected as expected at ~50 kDa molecular

weight from cells transfected with FX^{WT}, $FX^{Asp413Asp}$ and $FX^{Gly420Arg}$ and mocked transfected cells.

This FX protein bands represents the heavy chain of FX protein since the gel was performed under reducing conditions in the presence of (Beta-mercaptoethanol). No FX protein band could be detected in the lane loaded with cell lysates from mocked cells. GAPDH protein (~37kD) level was assessed in the same cell lysates as shown in the figure 3.4, This result shows no apparent difference in the expression of FX protein level in cells transfected with the various constructs

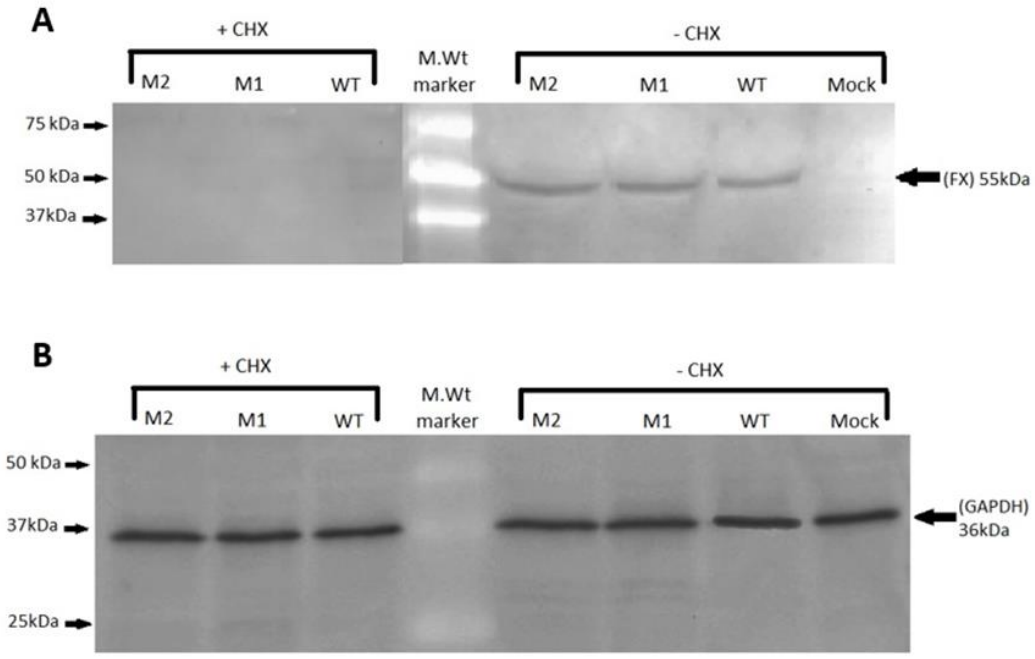

Figure 3.4: A. Western blot showing the expression of the FX protein (~ 50kD) in transfected cell lysates. The lanes indicated FXWT (WT), FXAsp413Asp (M1) and FXGly420Arg (M2) and non-transfected cells (Mock). B. The expression of the GAPDH gene (~37kD) is also shown. The protein size marker in kD is shown on the left side of the figure.

In comparison with other studies, our results were similar to the p. Ala275Val mutant studied in China, where FX protein was observed in the cell lysates of both the WT and p. Ala275Val mutant, in another study from Japan the following protein constructs were detected in transfected cell lysates WT, p.Gly154Arg, p.Val236Met, p.Gly263Val, p.Arg387Cys, p.Gly406Ser, p.Val424Phe and p.Gly406Ser/p.Val424Phe.

3.2.2. FX level in cell lysates:

The level of FX protein was measured in cell lysates of cells transfected with both recombinant mutants of FX (Asp413Asn, Gly420Arg) in comparison with WT form level in cells transfected with wild type FX. Figure 3.5 shows the level of $FX^{Gly420Arg}$ mutant was found to be similar to the FX^{WT} (44.354 ng/mL and 43.3

565 ng/mL respectively) (p value = 0.2), while a significant decrease was observed in case of the $FX^{Asp413Asn}$ mutant compared to the wild type (36.2705ng/mL and 43.3565 ng/mL respectively) (p value = 0.001).

In comparison with similar studies, in a study including multiple different missense mutations, FX antigen levels of p.Gly154Arg, p.Gly263Val,

p.Val424Phe, p.Gly406Ser/p.Val424Phe p.Val236Met, p.Arg387Cys and p.Gly406Ser were similar to the WT FX antigen level. (Nagaya, et al., 2018) While the p.Ala275Val mutant reported from China displayed a slight decrease in FX antigen levels in the cell lysate(61% of the WT FX: Ag) (Sun, 2016). These results confirm all the indicated mutations did not interfere with the production proteins in the cells.

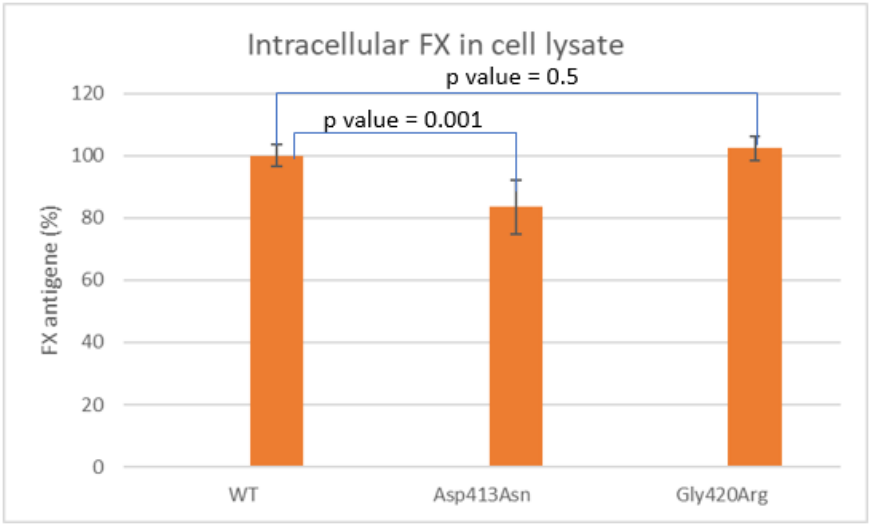

Figure 3.5: The level of WT FX and recombinant mutant proteins in cell lysates from transfected cells with the indicated recombinant constructs is shown as indicated in the figure.

3.3. FX level in culture media

The level of FX antigen in the conditioned culture media was evaluated by ELISA, as described in figure 3.6. The level of both mutants was compared with the wild type. FX^{WT} was found to be 0.933 ng/mL, while the $FX^{Gly420Arg}$ was similar to the WT (0.935 ng/mL) (p value = 0.5), while there was an increase in $FX^{Asp413Asp}$ mutant, was 1.318 ng/mL (p value = 0.3), shown in figure 3.6.

This indicates that both mutations did not affect the stability and secretion of the FX expressed proteins.

The effect of multiple FX missense mutations on the secretion of FX by measuring FX antigen levels in conditioning media, i.e. the antigen levels of the p.Gly154Arg, p.Gly263Val, p.Val424Phe and p.Gly406Ser/p.Val424Phe mutant proteins were significantly lower than the WT level. While no significant change detected for the p.Val236Met, p.Arg387Cys and p.Gly406Ser mutant proteins. (Nagaya, et al., 2018)

In another two studies the p.Met402Thr mutant was found to be 25% of the expressed WT FX level in culture media. (Chikasawa, et al., 2014) However, the p.Ala275Val mutant was significantly decreased in the culture media to 3.47% compared to the WT FX antigen levels in supernatant media. (Sun, 2016)

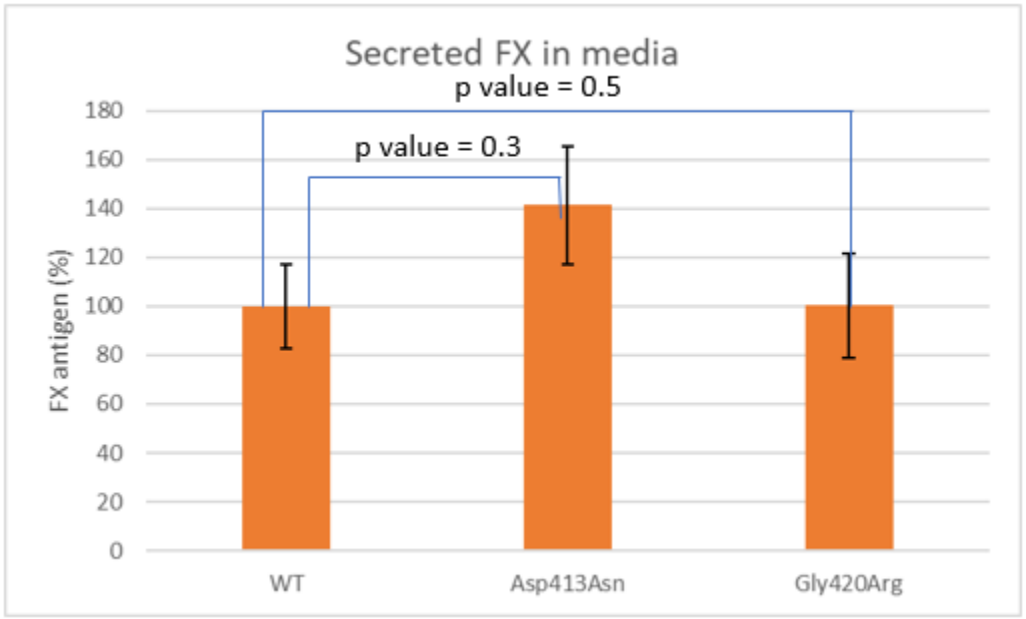

Figure 3.6: The level of WT FX and recombinant mutant proteins in con from transfected cells with the indicated recombinant constructs is shown as indicated in the figure.

3.4. FX activity in culture media

In parallel, the recombinant FX activity of the mutants in the culture media was evaluated by comparing PT results of 10X concentrated media mixed 1:1 with FX deficient plasma. When the WT FX activity was set to 100%, the Asp413Asn mutant was 25.9% while the Gly420Arg mutant was only 31.4% in comparison to the WT FX as described in figure 3.7.

These results showed the integral protein detected by ELISA had significant lower activity in comparison to the WT protein.

Previous reports describing other FX mutant's activity compared with the wild type FX activity in the culture media showed similar results. The study from China showed the p.Ala275Val mutant had decreased to about 8% of the wild type activity based on PT measurements. (Sun, 2016)

Based on the study from Japan, the p.Met402Thr mutant had 7.7% activity compared to the wild type based on PT method. (Chikasawa, et al., 2014) Another study from Japan investigating the effect different mutants on FX activity found that all the mutants investigated (p.Gly154Arg, p.Gly263Val, p.Val424Phe, p.Gly406Ser/p.Val424Phe p.Val236Met, p.Arg387Cys and p.Gly406Ser) revealed significant decrease in FX activity (20% and less) compared to the wild type activity (Nagaya, et al., 2018).

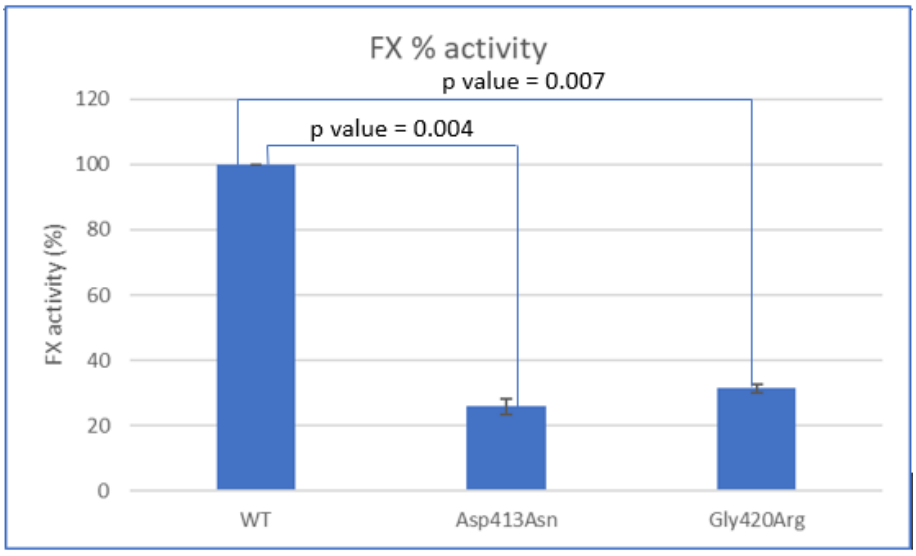

Figure 3.7: FX% activity in culture media showing significant decrease in FX protein activity in both mutants (Asp413Asn and Gly420Arg) compared to the WT, using one-stage PT-based method.

3.5. *F10* expression.

Total RNA was extracted from HEK293T cells transfected with FX^{WT}, $FX^{Gly420Arg}$ and $FX^{Asp413Asn}$ recombinant constructs. Real time-PCR was used to quantify the *F10* mRNA expression level of from the three variants recombinant vectors, *F10* expression was normalized with Beta actin.

The results from two independent tests showed no significant difference in *F10* mRNA from the three recombinant vectors, as shown in figure 3.8.

These results indicate the two indicated mutations in our study did not seem to affect the stability of *F10* RNA.

The expression level of the mutant p.Ala275Val was reported in a previous study, a 1.8-fold increase in *F10* mRNA expression level compared to the wild type. (Sun, 2016)

Figure 3.8 *F10* expression levels (relative value) RT-PCR analysis of F10 mRNA levels from transfected cells with the indicated recombinant constructs and mocked control cells is shown as indicated in the figure.

3.6. Bioinformatic prediction and analysis of Asp413Asn mutant:

Bioinformatic tools used to predict the impact of the Asp413Asn mutation as follows

- PolyPhyn-2 predicted the Asp413Asn mutation to be probably damaging with a score of 1.000, the report is shown in figure 3.9.

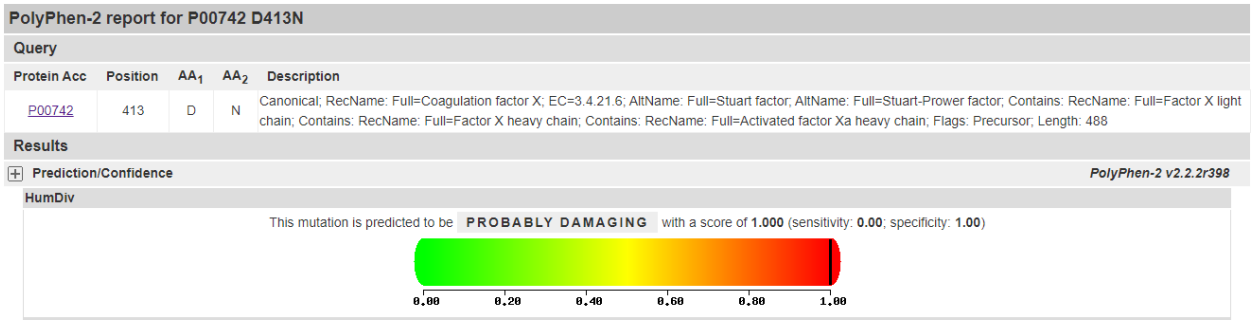

Figure3.9 PolyPhen-2 report the Asp413Asn mutation indicating the mutation to be probably damaging with a score of 1.000

- SIFT and PROVEAN reported the mutation as deleterious and damaging respectively, the report is presented in figure 3.10.

VARIATION		PROTEIN SEQUENCE CHANGE				PROVEAN PREDICTION				SIFT PREDICTION			
ROW_NO.	INPUT	PROTEIN_ID	POSITION	RESIDUE_REF	RESIDUE_ALT	SCORE	PREDICTION (cutoff=-2.5)	#SEQ	#CLUSTER	SCORE	PREDICTION (cutoff=0.05)	MEDIAN_INFO	#SEQ
1	P00742 413 D N	P00742	413	D	N	-4.81	Deleterious	171	30	0.000	Damaging	2.76	104

Figure 3.10: SIFT and PROVEAN report for mutant Asp413Asn predicted the mutation to be Damaging (score 0.000) and Deleterious (-4.51) respectively.

- HOPE predicted the indicated mutation is probably damaging to the protein based on conservation scores, since the mutation is located in an important domain for protein activity and in contact with other domains involved in protein activity, so this mutation is predicted to affect protein function, models demonstrating the predicted change in structure are shown in figures 3.11 and 3.12.

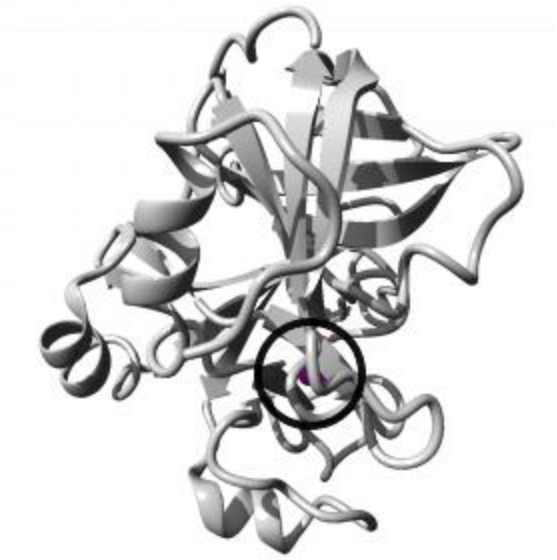

Figure 3.11: Structure of FX in ribbon-presentation. The protein is colored gray and the side chain of the mutated amino acid (Asp413Asn) is colored magenta (indicated in the circle).

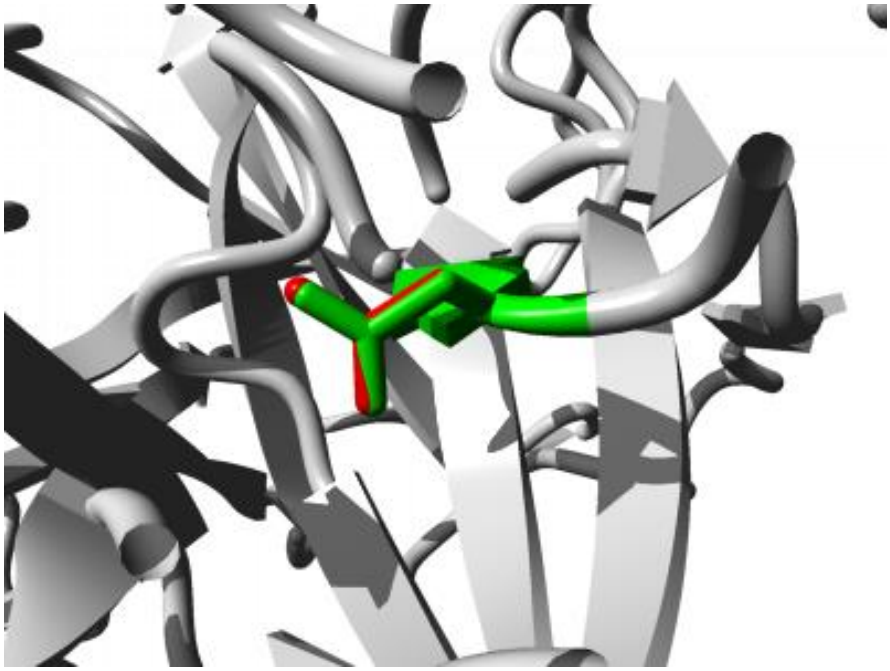

Figure 3.12 Close-up to the mutation site. The protein is colored gray the side chain of the wild type protein is colored green and the side chain of the Asp413Asn is colored red

3.7.Bioinformatic prediction and analysis of Gly420Arg:

In order to predict the impact of the mutation Gly420Arg, the same bioinformatic tools were used, and the results were as follows:

- PolyPhyn-2 predicted the mutation Gly420Arg to be probably damaging with a score of 1.000, prediction results shown in figure 3.13.

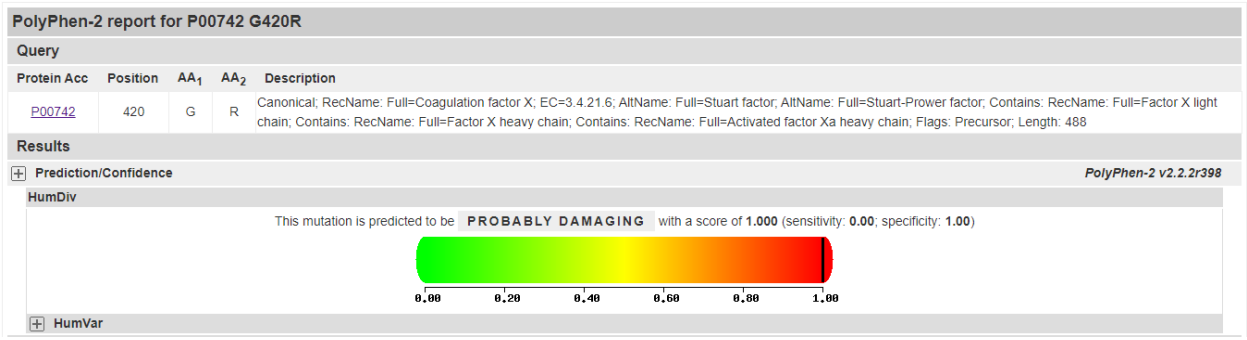

Figure.3.13: PolyPhen-2 report of Gly420Arg predicting the mutation to be probably damaging with a score of 1.000

- SIFT and PROVEAN reported the mutation as deleterious and damaging respectively, as shown in figure 3.14.

VARIATION		PROTEIN SEQUENCE CHANGE				PROVEAN PREDICTION				SIFT PREDICTION			
ROW_NO.	INPUT	PROTEIN_ID	POSITION	RESIDUE_REF	RESIDUE_ALT	SCORE	PREDICTION (cutoff=-2.5)	#SEQ	#CLUSTER	SCORE	PREDICTION (cutoff=0.05)	MEDIAN_INFO	#SEQ
1	P00742 420 G R	P00742	420	G	R	-7.70	Deleterious	171	30	0.000	Damaging	2.76	104

Figure 3.14: SIFT and PROVEAN report for mutant Gly420Arg predicted the mutation to be Damaging (score 0.000) and Deleterious (-7.70) respectively.

- HOPE analysis suggested that the amino acid substitution from neutral glycine to the positively charged Arginine with a bulky side chain that could lead to local structure changing in the surrounding area which is very close to the active site. predicted changes in protein structure are shown in figures 3.15 and 3.16

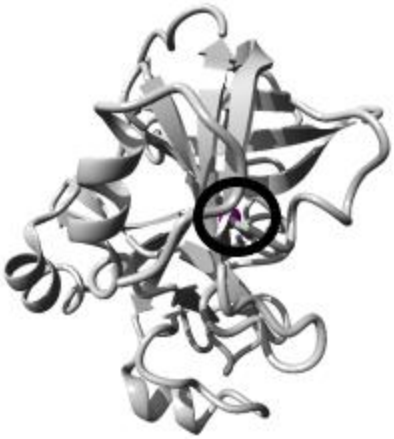

Figure 3.15: Structure of FX in ribbon-presentation. The protein is colored gray and the side chain of the mutated amino acid (Gly420Arg) is colored magenta (indicated in the circle).

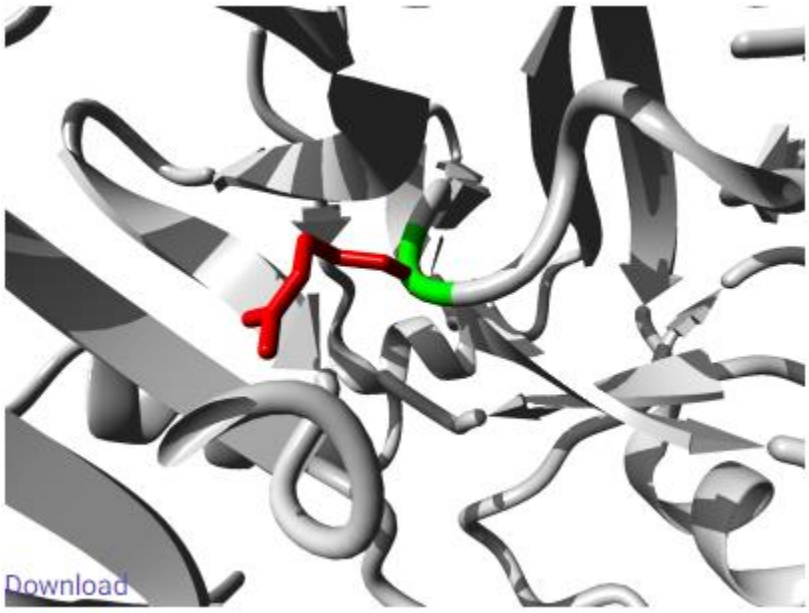

Figure 3.16: Close-up to the mutation site, the protein is colored gray the side chain of the wild type protein is colored green and the side chain of the Asp413Asn is colored red

3.8. Conservation studies of Asp413 and Gly420

3.8.1. Conservation analysis of Asp413 position of FX illustrated that it was conserved in homologues species. as shown in figure 3.17.

Figure 3.17: Conservation analysis of Asp413 showing that this position was conserved among various homologues species

3.8.2. Conservation analysis of Gly420 position of FX illustrated that it was conserved in homologues species as shown in figure 3.18.

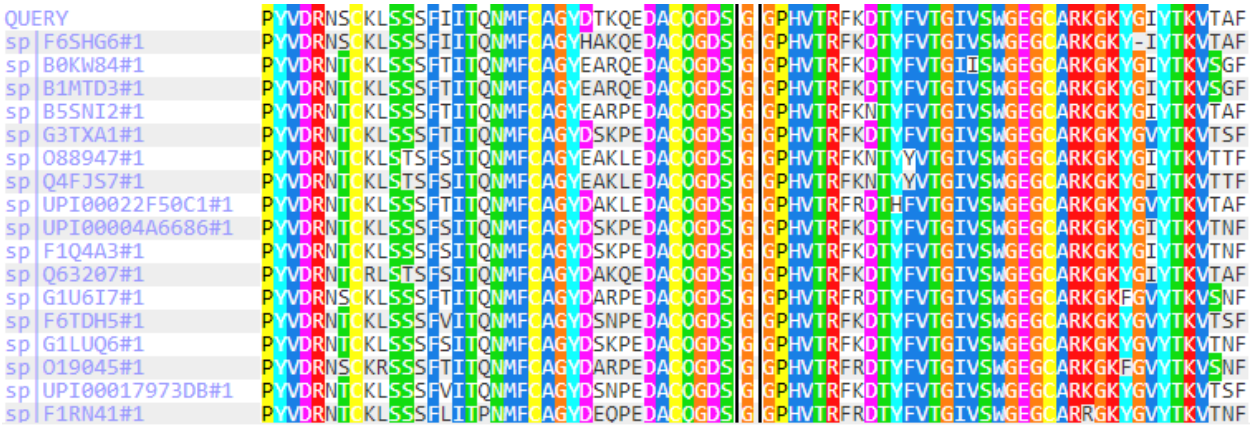

Figure.3.18: conservation analysis of Gly420 the position was conserved among homologous species

3.8.3. Conservation analysis with paralog serine proteases showed that both Asp413 and Gly420 were conserved and shared between various vitamin k dependent serine proteases, results are presented in table 3.1

Table 3.1 Sequence alignment of various vitamin k dependent serine proteas clotting factors showed that both Asp413 and Gly420 positions are conserved. Conserved amino acids are depicted in bold, Asp413 and Gly420 are highlighted.

Protein	Sequence
FX	QE**D**A**C**Q**GDSG**G**P**
FVII	SK**D**S**C**K**GDSG**G**P**
FIX	GR**D**S**C**Q**GDSG**G**P**
Prothrombin	RG**D**A**C**E**GDSG**G**P**
Protein C	RQ**D**A**C**E**GDSG**G**P**

The bioinformatic structure prediction and conservation analysis results for both the Asp413Asn and Gly420Arg were similar to those from other reports, that used the same tools to predict the impact of missense mutations on FX proteins, for example PolyPhen-2 report for the p.Cys81Arg and p.Cys81Tyr mutants studied in China were all predicted to be probably damaging with a score 0.999 for each, the other Ala275Val also reported in China was also predicted to be probably damaging.

The same was also observed in conservation studies, where all the investigated mutations detected in FX deficiency patients were found to be located in conserved locations using multiple tools for multiple sequence alignment in multiple homologous species.

4. Discussion.

In the present study we investigated the molecular and structural consequence of specific missense mutation in the factor X gene leading to severe FX loss of activity. This mutation was previously reported in Palestinian FX deficiency patient, who suffered from severe bleeding disorder since birth. FX activity was evaluated by measuring PTT and PT which indicated major decreased coagulant activity.

Genetic analysis of the *F10* gene in this patient revealed a missense mutation caused by G>A transition in exon 8 leading to the novel Asp413Asn mutation.

In parallel, similar analysis was applied to another previously identified missense mutation involving Gly420Arg which lead to coagulation deficiency.

The novel Asp413Asn mutant was the only reported in this location in the Palestinian population, and was predicted to have major impact on the structure of FX protein, due to the nature of shift in amino acid from negatively charged to neutral side chain and its location close to the catalytic domain of FX.

Conservation analysis of both Asp413 and Gly420 among multiple species revealed that these amino acids are highly conserved in FX protein and other serine proteases. This strongly suggest that both amino acids in their relevant locations are crucial for FX activity, similar to other missense mutations (Nagaya, et al., 2018), (Sun, 2016), (Jin Y, 2018).

This is highly supported by bioinformatic prediction tools (PolyPhen-2, PROVEAN, SIFT and HOPE), all indicating these mutations to be damaging due to their significant distortion of protein structure and function, similar to other previously reported missense mutations (Chikasawa, et al., 2014) (Jin Y, 2018) (Nagaya, et al., 2018) (Sun, 2016).

Recombinant protein expression system was used to understand the molecular mechanism of FX insufficiency due to the indicated Asp413Asn and Gly420Arg mutations; the Asp413Asn mutant protein was detected in cell lysate with slight reduction of FX protein was observed, while the Gly420Arg mutant was detected in the cell lysate with no significant difference in FX protein level. Which indicates that these mutations did not affect protein stability.

This is similar to previous reports of other missense mutations in the *F10* gene (Chikasawa, et al., 2014) (Nagaya, et al., 2018) (Sun, 2016)

FX activity evaluated by PT based assay revealed a great reduction in FX coagulant activity (25%) compared with the wild type, while FX protein level in the culture media was increased.

FX activity in the culture media of the Gly420Arg construct was found to be decrease to 31% compared to FX activity of the wild type, while no difference was observed in FX protein in the culture media.Which indicates that the mutants Asp413Asp and Gly420Arg did not block the secretion of the protein outside the cell, with significant loss of its functional activity.

This was similar among all other investigated missense mutants of FX where the protein activity was decreased at variable levels. But the level of secreted FX Proteins in the culture media was found to be decreased in other missense mutations. (Sun, 2016) (Nagaya, et al., 2018)

Consistently this is further supported with *F10* expression results that showed no significant difference in *F10* mRNA of the Asp413Asn and Gly420Arg mutants compared to the wild type.

Compared with other studies that investigated the impact of other missense mutations on *F10* expression, unlike our results for the Asp413Asn and Gly420Arg, it was reported that the expression of the Ala175Val mutant was 1.6 folds increased compared to the expression of the wild type. (Sun, 2016)

In other studies that used the same technique to understand the functional implications of specific mutations it was found that Gly668Asp led to destabilization of EPHA2 receptor, changed the subcellular localization and altered its activation, (Zhai, Zhu , Li, & Yao, 2019) while for Interferon Beta the investigated mutations showed increased protein and mRNA production.

References

Adzhubei IA, S. S. (2010). A method and server for predicting damaging missense mutations. *Nat Methods*.

Chafa, O. (2009). Characterization of a homozygous Gly11Val mutation in the Gla domain of. *Thrombosis Research*, 144-149.

Chikasawa, Y., Shinozawa, K., Amano, K., Ogata, K., Hagiwara, T., Suzuki, T., . . . Fukutake, K. (2014). Factor X M402T: a homozygous missense mutation identified as the cause of cross-reacting material-reduced deficiency. *Int J Hematol*.

F. H. HERRMANN, G. A.-S. (2008). Factor X deficiency: clinical manifestation of 102 subjects from Europe and Latin America with mutations in the factor 10 gene. *Haemophilia*, 479-489.

Falls, L. A., Furie, B. C., Jacobs, M., Furie, B., & Rigby, A. C. (2001). The ω-Loop Region of the Human Prothrombin γ-Carboxyglutamic Acid Domain Penetrates Anionic Phospholipid Membranes. *Journal of Biological Chemistry*, 23895-23902.

Hanka Venselaar, T. A. (2010). Protein structure analysis of mutations causing inheritable diseases. An e-Science approach with life scientist friendly interfaces. *BMC Bioinformatics.*

Hoffbrand, A. V., & H. Moss, P. A. (2011). *Essential Haematology.* Wiley-Blackwell.

HOUGIE, C. (1957). STUART CLOTTING DEFECT. I. SEGREGATION OF AN HEREDITARY. *journal of clinical investigation*, 485-496.

Jin Y, C. X. (2018). A novel factor X mutation Cys81 by Arg and a reported factor VII polymorphism Arg353 replaced by Gln co-occured in a patient. *Blood Coagul Fibrinolysis*.

Karimi, M., Menegatti, M., Menegatti, M., Afrasiabi, A., & Flora, P. (2008). Phenotype and genotype report on homozygous and heterozygous patients with congenital factor X deficiency. *Haematologica*, 934-938.

Kaul, R. K., Hildebrand, B., Roberts, S., & Jagadeeswaran, P. (1984). Isolation and characterization of human blood-coagulation factor X cDNA. *Gene*, 311-314.

LC, N. (2008). Sample prep for proteomics of breast cancer: proteomics and gene ontology reveal dramatic differences in protein solubilization preferences of radioimmunoprecipitation assay and urea lysis buffers. *Proteome Sci*.

Leytus, S. P., Foster , D. C., Kurachi , K., & Earl , D. W. (1986). Gene for Human Factor X: A Blood Coagulation Factor Whose Gene Organization Is Essentially Identical with That of Factor IX and Protein Ct. *Biochemistry*, 5098-5 102.

Nagaya, S., Akiyama, M., Murakami, M., Sekiya, A., Asakura, H., & Morishita, E. (2018). Congenital coagulation factor X deficiency: Genetic analysis of five patients and functional characterization of mutant factor X proteins. *Haemophilia*, 1-12.

NCBI. (2019, November 11). *COBALT*. Retrieved from NCBI: https://www.ncbi.nlm.nih.gov/tools/cobalt/re_cobalt.cgi

Norouzi , R., Hojati, Z., & Dehbashi, M. (2018). In vitro and computational studies on the effects of ARE deletion and targeted mutations on the expression of interferon beta-1a in HEK293T cells. *APPLIED GENETICS AND MOLECULAR BIOTECHNOLOGY*.

Padmanabhan, K. (1993). Structure of Human Des(1-45) Factor Xa at 2·2 Å Resolution. *Journal of Molecular Biology*, 947-966.

Perez-Pujol, S. (2012). Factor V Leiden and Inflammation. *Thrombosis*, 2.

Shinohara, K. (2008). A case of factor X (FX) deficiency due to novel mutation V196M, FX Hofu. *International Journal of Hematology*, 256-259.

Smoom, R., Abushkedim , I., & Darwish, H. (2015). Identification of two Novel Mutations in the Factor X Gene; A 5' Donor SpliceSite Mutation (IVS1+1G**>** T) and a Missense Mutation (Asp413Asn G>T) in Unrelated Palestinian Factor X Deficient Patients. *Blood Disorders & Transfusion*, 1-6.

Sun, N. (2016). A novel Ala275Val mutation in factor X gene influences its structural compatibility and impairs intracellular trafficking and coagulant activity. *Thrombosis Research*, 108-113.

SUTTIE, J. W. (1993). Synthesis of vitamin K-dependent proteins. *FASEB*, 445-452.

Telfer, T. P. (1956). A ‘New’ Coagulation Defect . *British Journal of Haematology*, 308-316.

The Human Gene Mutation Database. (2019, 11 14). Retrieved from HGMD: http://www.hgmd.cf.ac.uk/

Yongwook Choi, G. E. (2012). Predicting the Functional Effect of Amino Acid Substitutions and Indels. *PLOS ONE*.

Zhai, Y., Zhu , S., Li, J., & Yao, K. (2019). A Novel Human Congenital Cataract Mutation in EPHA2 Kinase Domain (p.G668D) Alters Receptor Stability and Function. *Lens*, 4717-4726.

الملخص

العامل العاشر في سلسله تخثر الدم هو ا حد بروتيازات السيرين المعتمده على فيتامين ك، يصنع في الكبد وله دور محوري في سلسله تخثر الدم. يتم تنشيط هذا البروتين عن طريق اما المسار الخارجي او الداخلي، حيث يشكل العامل العاشر المكون الرئيسي في مجمع البروثرومبيناز الذي يعمل على تحويل البروثرومبين الى ثرومبين.

العامل العاشر مشفر بواسطه جين موجود على الكروموسوم الثالث عشر، يتكون جين العامل العاشر من ثمان اكسونات و سبع انترونات يشفر لبروتين يتكون من 488 حمض اميني، حتى الان اكثر من 130 طفره تم الابلاغ عنها في هذا الجين، معظها كانت من نوع الطفرات المغلطه. يتم تصنيف مرضى نقص العامل العاشر بناء على مستوى البروتين بالدم و مدى فعاليه الوظيفه الانزيميه للبروتين مرضى النوع الاول يعانون من نقص في كميه البروتين في الدم، بينما مرضى النوع الثاني يوجد لديهم بروتينات غير فعاله.

مؤخرا تم تشخيص مريضين بنقص العامل العاشر و تم التعرف على الطفرات لكل منهما حيث كانت طفرات جديده لم يتم ذكرها سابقا في الادب العلمي، كان احدها الطفره المغلطه التي نتج عنها استبدال حمض الاسبارتات بالاسبارجين في الموقع رقم 413، الهدف من دراستنا هو التعرف على الاثار الجزيئيه والبنائيه المترتبه على هذه الطفره.

تم احداث طفرات على الجين الكامل الطبيعي باستخدام تقنيه الطفرات الموجهه للموقع للحصول على ما يمثل الطفره التي تم تشخيصها لدى مريض فلسطيني بنقص العامل العاشر، بجانب ذلك تم دراسه طفره اخرى مغلطه تم ذكرها سابقا بنفس الطريقه، تم ادخال الجين الطبيعي بالاضافه الى الجينين اللذان يحتويان على الطفرات في خلايا جذعيه جنينيه كل على حده، تمت دراسه التحليل الغربي لفصل البروتينات، حيث

لم يتبين ان لهتين الطفرتين تاثير واضح على كميه البروتين، فعاليه الانزيم تم قياسها من خلال نتائج وقت البروثرومبين لبروتينات العامل العاشر المفرز من الخلايا و بدا ان البروتينات قد فقدت جزء كبيرا من فعاليتها الانزيميه، تم كذلك دراسه مدى تاثر الحمض النووي الريبوزي غير منزوع الاكسجين (الرنا) ، حيث وجدنا ان لا تاثير يذكر لهذه الطفرات على عمليه نسخ الجين و استقرار جزيئات الرنا ، قمنا كذلك باستخدام تطبيقات المعلوماتيه الحيويه للتنبؤ بمدى تاثير هذه الطفرات على بناء البروتين و استقراره، وقد كانت نتائج البرامج المستخدمه جميعها ان الطفرات ذات تاثير تدميري على بناء و وظيفه البروتين بسبب قرب الطفرات من موقع ارتباط ايونات الصوديوم.

ختاما يبدو ان لهذه الطفرتين تاثير محدود بموقعهما في البروتين بحيث يكون لا يتاثر انتاج البروتين ولكن البروتينات المنتجه تكون ذات فعاليه ضئيله، و يكون اصحاب هذه الطفرات مرضى نقص العامل العاشر من النوع الثاني.